Supplemental Information

Affinity-Directed Dynamics of Host–Guest Motifs for Pharmacokinetic Modulation *via* Supramolecular PEGylation

Caitlin L. Maikawa,[a] Andrea I. d'Aquino,[b] Eric T. Vuong,[a] Bo Su,[c] Lei Zou,[c] Peyton C. Chen,[a] Leslee T. Nguyen,[d] Anton A. A. Autzen,[b,e,f] Joseph L. Mann,[b] Matthew J. Webber,[c,*] Eric A. Appel[a,b,g,h*]

Table of Contents

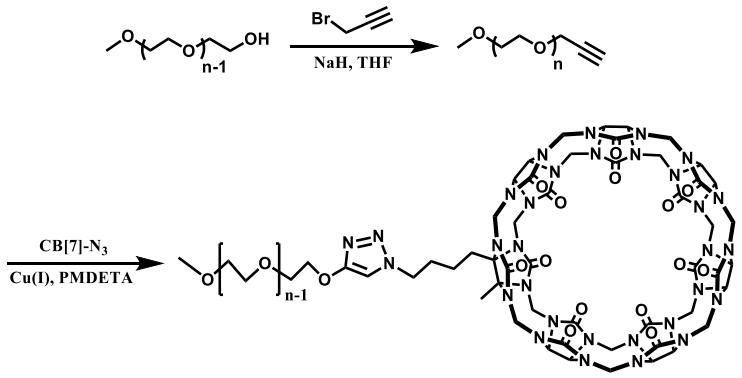

Figure S1. Synthesis of cucurbit[7]uril-PEG_{20k}.

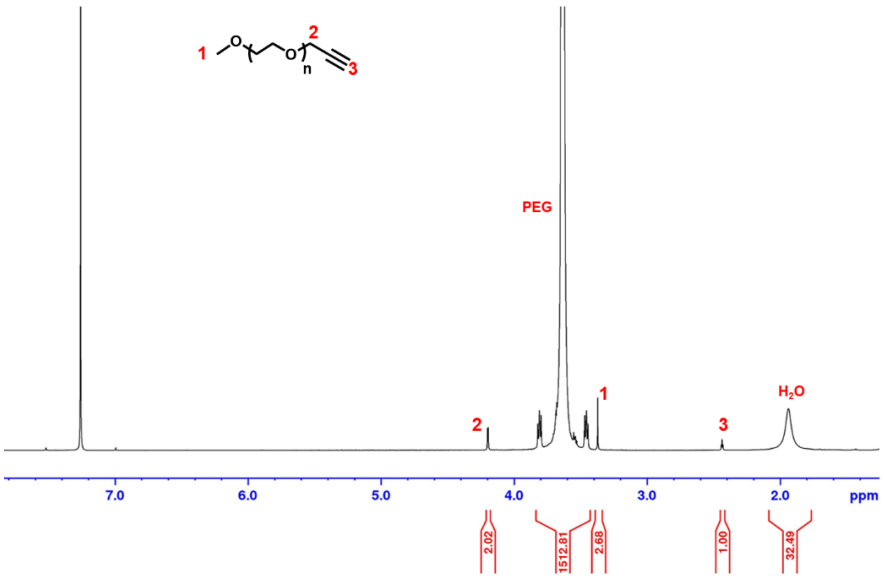

Figure S2. H^1 NMR (400 MHz, $CDCl_3$, 298K) for poly(ethylene glycol)$_{20k}$-alkyne ($mPEG_{20k}$-Alkyne). Residual H_2O ~94 mol%.

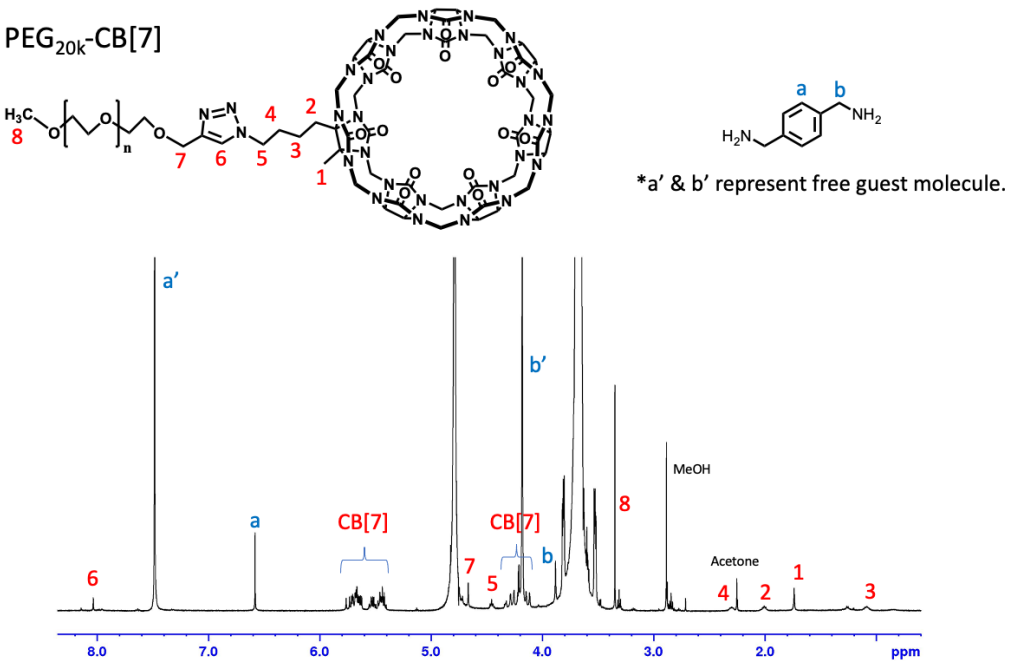

Figure S3. H^1 NMR (500 MHz, D_2O, 298K) for poly(ethylene glycol)$_{20k}$-cucurbit[7]uril (mPEG$_{20k}$-CB[7]), with p-xylylenediamine added to the sample to aid visualization of CB[7] by NMR. Residual MeOH ~64 mol% and residual acetone ~9 mol%.

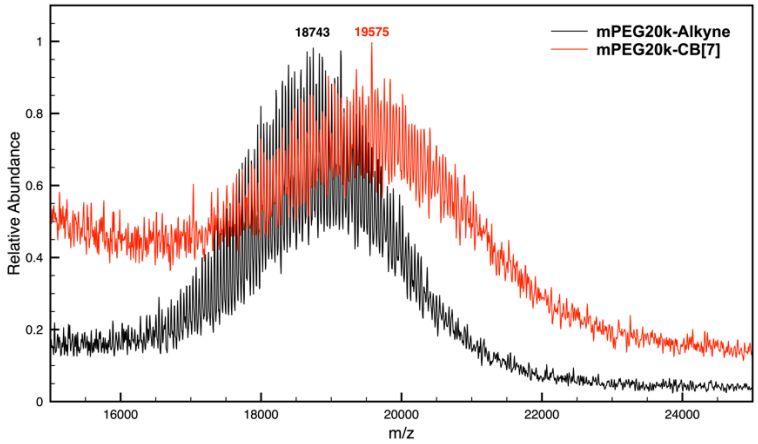

Figure S4. MALDI-MS (Bruker Xtreme MALDI-TOF-TOF, 2.5 dihydroxybenzoic acid matrix) for mPEG$_{20k}$-Alkyne and mPEG$_{20k}$-CB[7] with the peak of maximum abundance labelled in each. Expected MW increase for CB[7] addition via "click" is +1274.

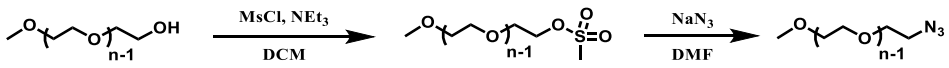

Figure S5. Synthesis of azide-PEG_{20k}

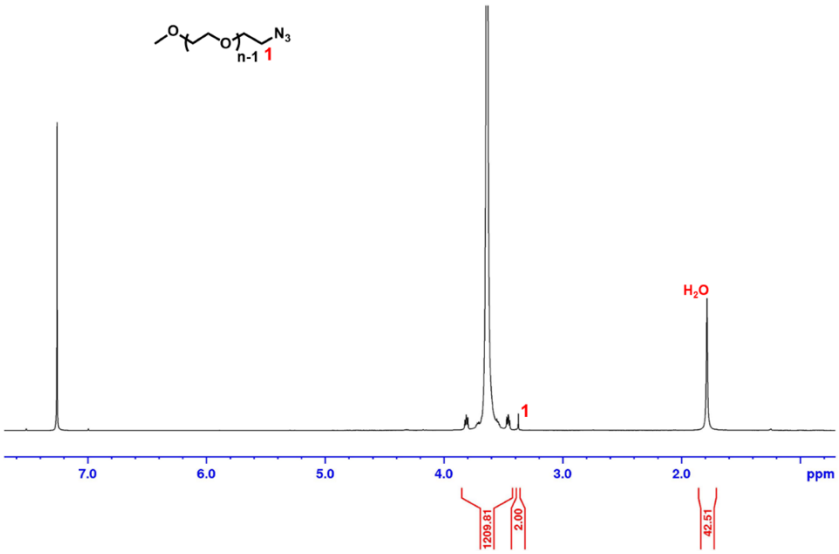

Figure S6. H^1 NMR (400 MHz, $CDCl_3$, 298K) for poly(ethylene glycol)$_{20k}$-azide ($mPEG_{20k}$-N_3). Residual H_2O ~95 mol%.

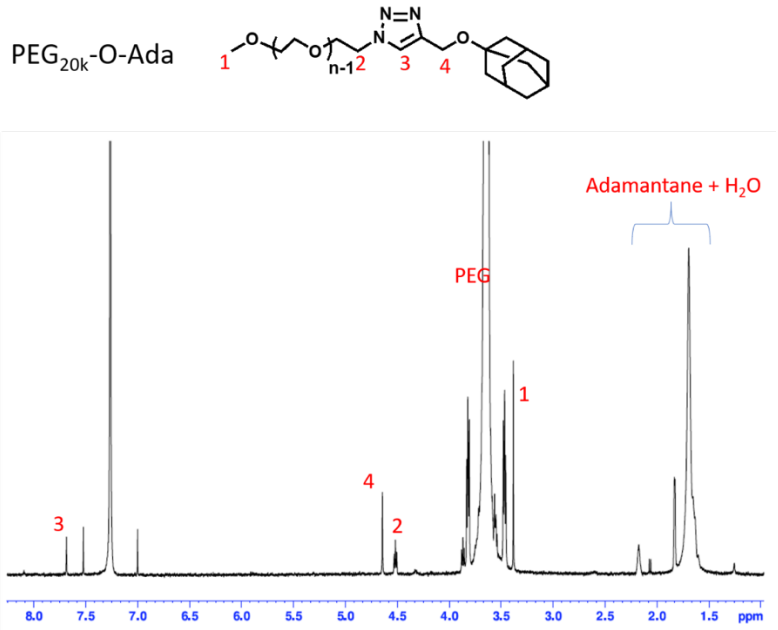

Figure S7. H^1 NMR (400 MHz, $CDCl_3$, 298K) for poly(ethylene glycol)$_{20k}$-O-adamantane (PEG_{20k}-O-Ada). Residual H_2O ~93 mol%.

Figure S8. Synthesis of O-adamantane-PEG_{20k}

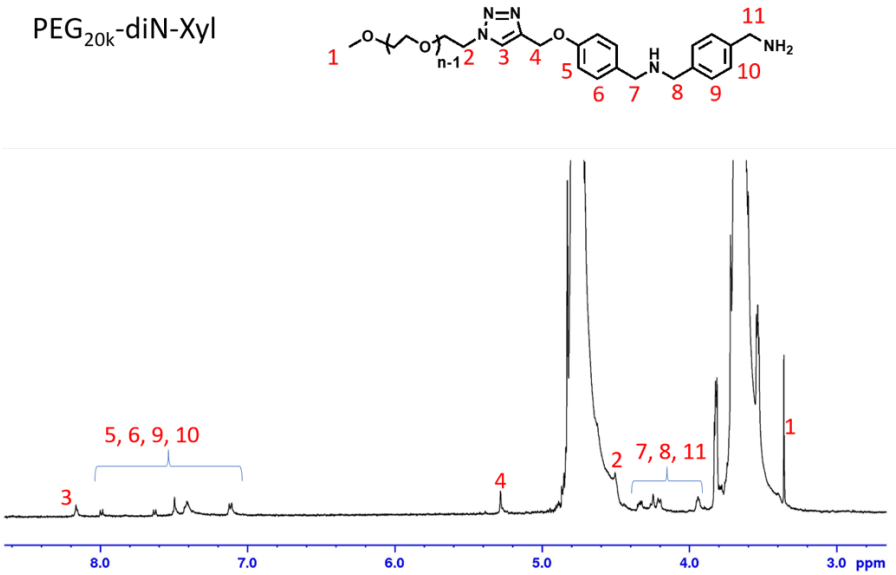

Figure S9. H^1 NMR (400 MHz, D_2O, 298K) for poly(ethylene glycol)$_{20k}$-xylylenediamine (PEG_{20k}-Xyl).

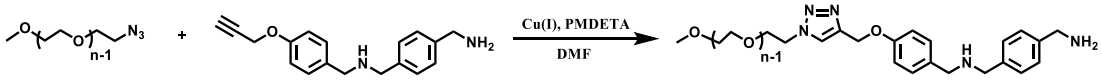

Figure S10. Synthesis of p-xylylenediamine-PEG_{20k}.

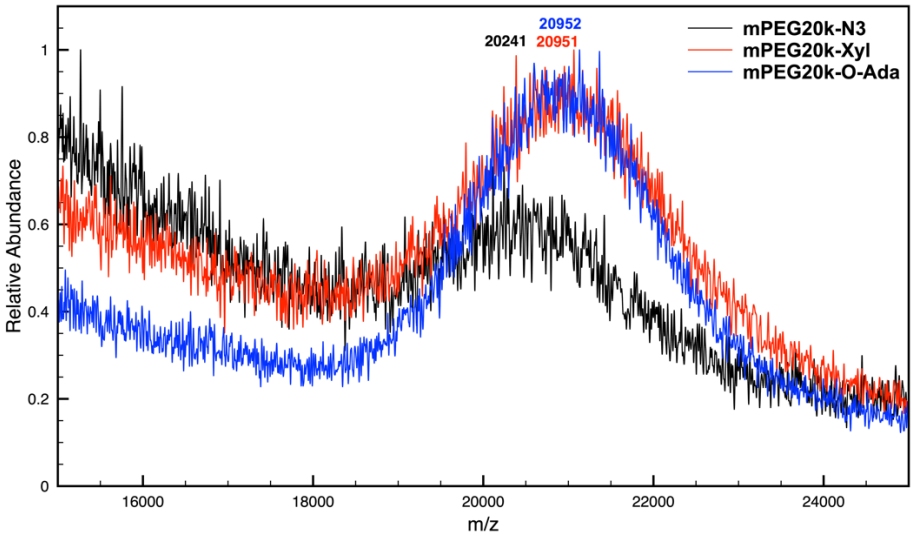

Figure S11. MALDI-MS (Bruker Xtreme MALDI-TOF-TOF, 2.5 dihydroxybenzoic acid matrix) for $mPEG_{20k}$-N_3, $mPEG_{20k}$-Xyl, and $mPEG_{20k}$-O-Ada with the peak of maximum abundance labelled in each. Expected MW increase for Xyl addition *via* "click" is +280 while that for O-Ada addition via "click" is +190.

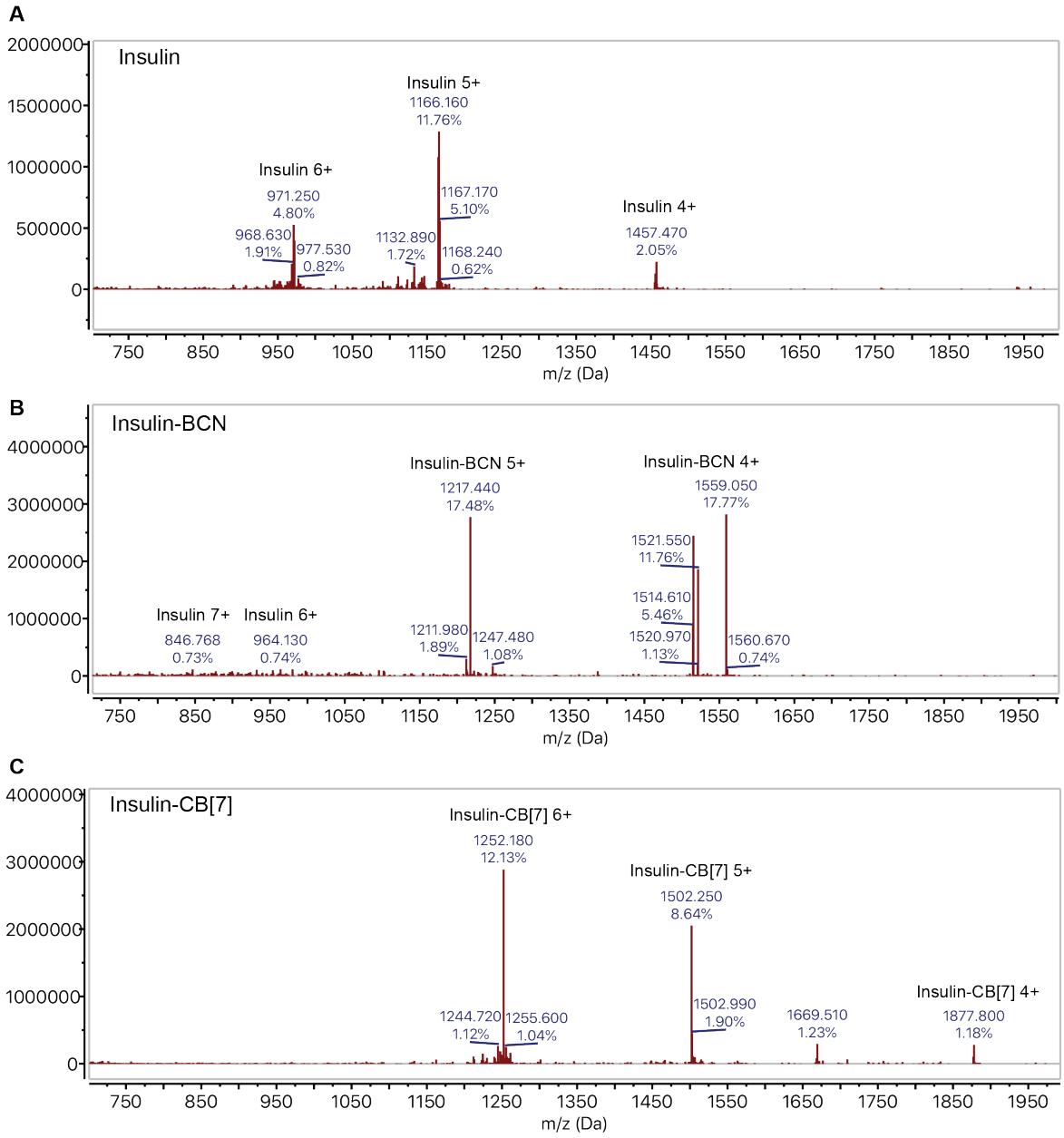

Figure S12: Liquid Chromatography Mass Spectrometry of insulin and insulin conjugates. Thermo Exactive Orbitrap Liquid Chromatography Mass Spectrometry instrument was used to obtain Low resolution spectra of **(A)** insulin, **(B)** insulin-BCN, **(C)** Insulin-CB[7].

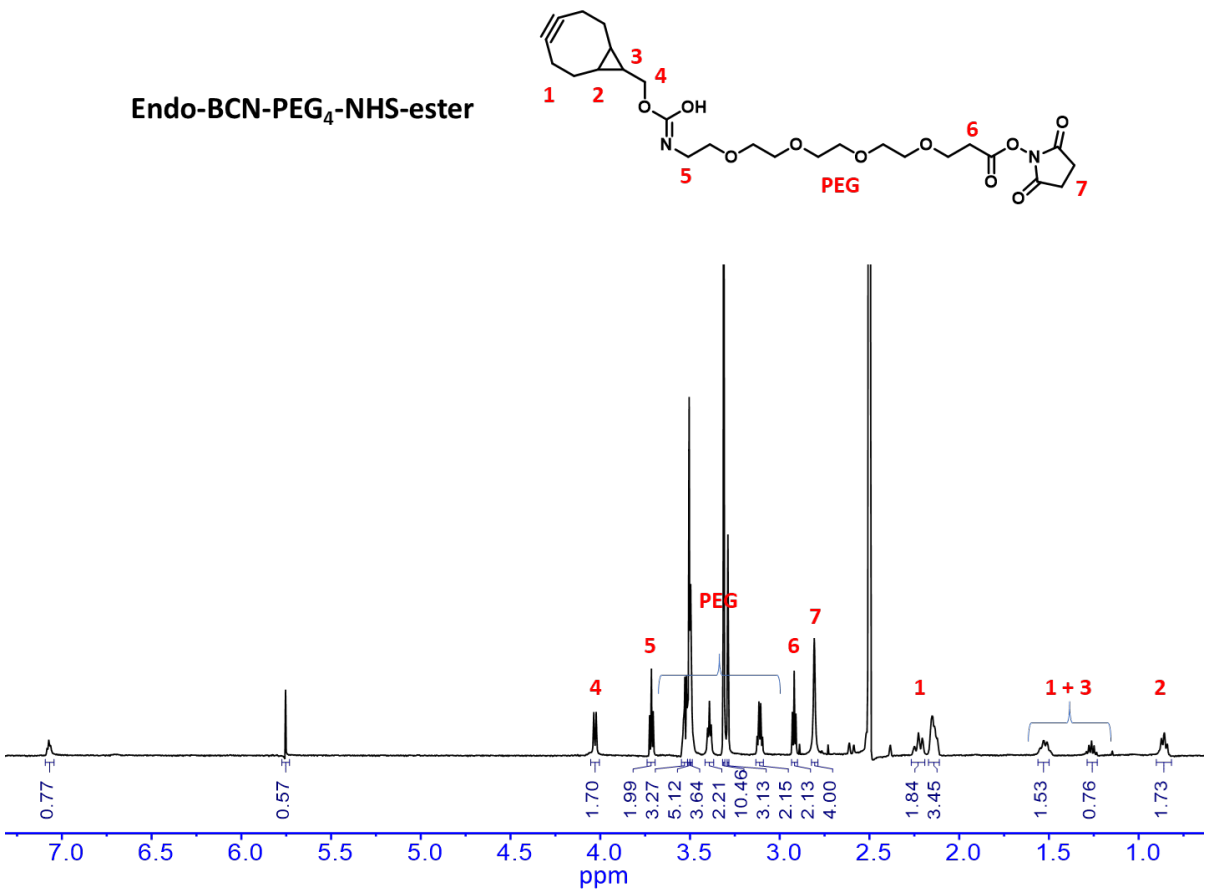

Figure S13. H^1-NMR (600 MHz, DMSO-d_6, 298 K) of endo-BCN-PEG_4-NHS-ester.

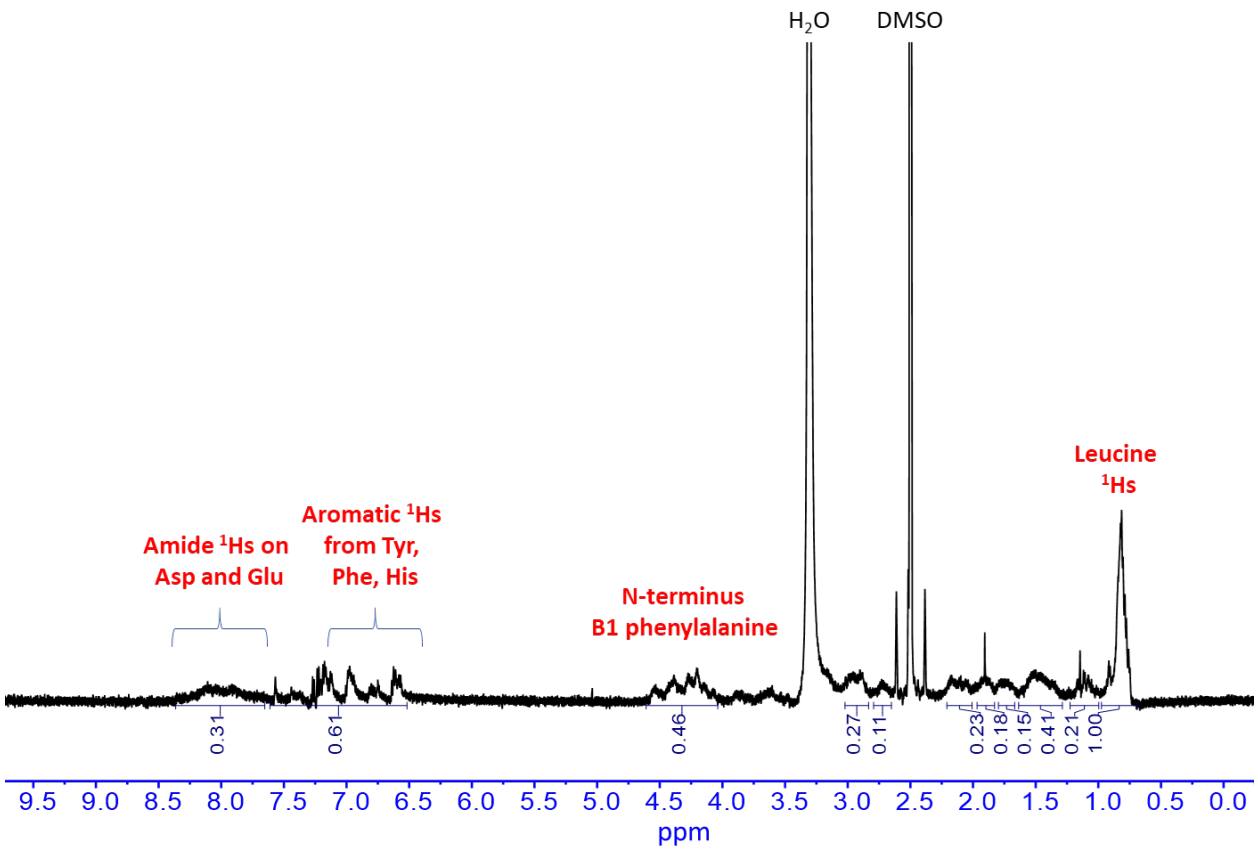

Figure S14. H^1-NMR (600 MHz, DMSO-d_6, 298 K) of insulin.

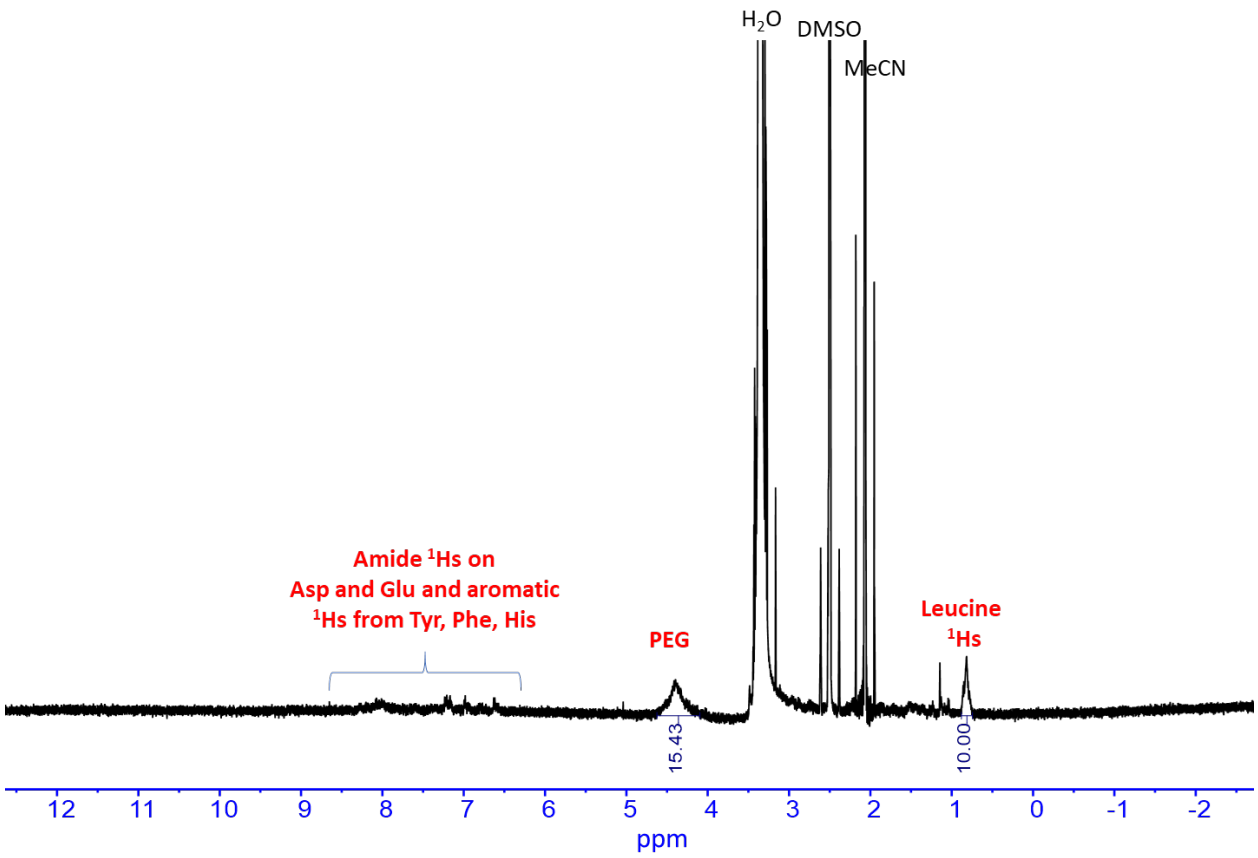

Figure S15. H^1-NMR (600 MHz, DMSO-d_6, 298 K) of BCN-functionalized insulin.

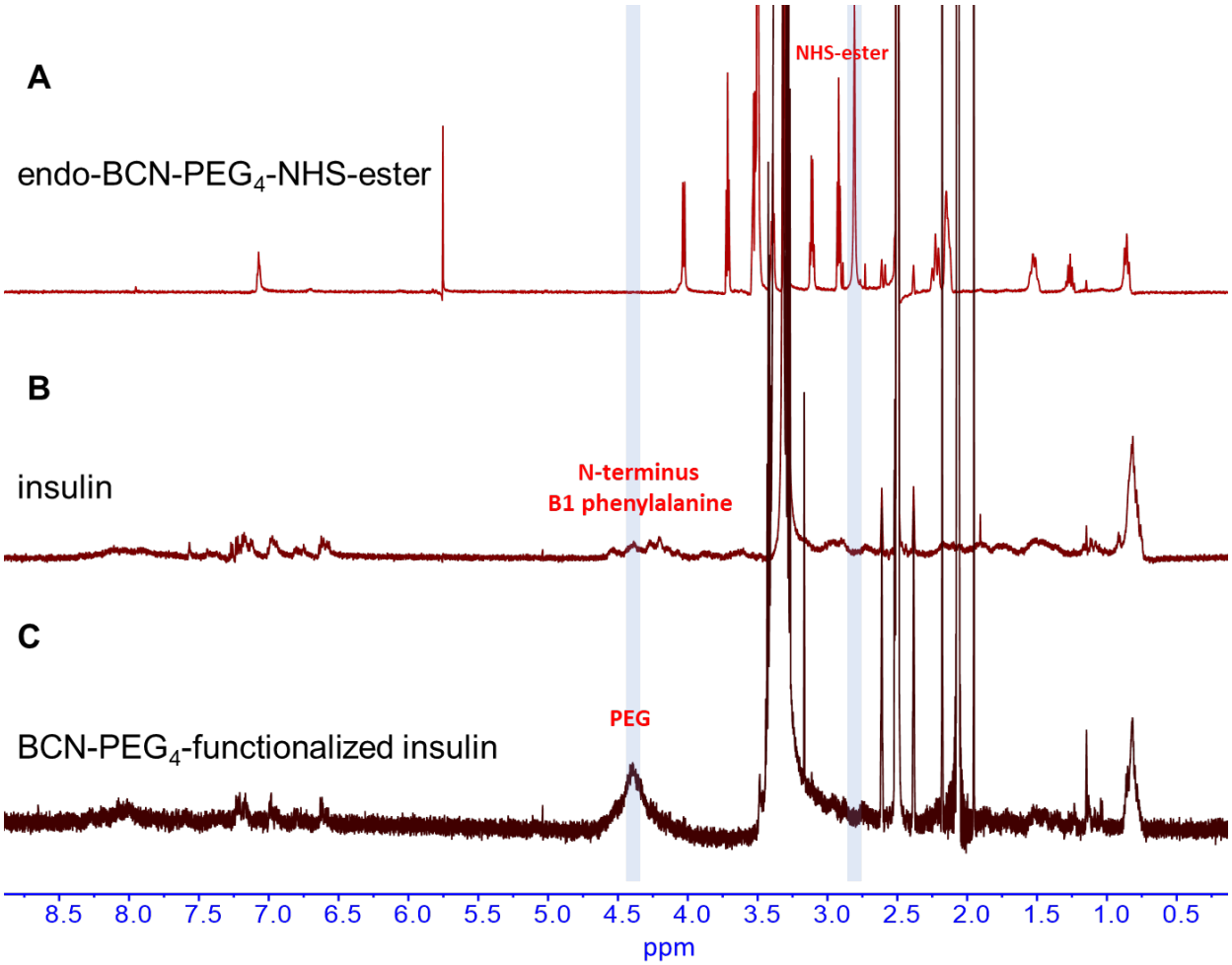

Figure S16. ^{1}H-NMR (600 MHz, DMSO-d_6, 298 K) of **(A)** endo-BCN-PEG$_4$-NHS-ester, **(B)** insulin and **(C)** BCN-PEG$_4$-functionalized insulin. The disappearance of the NHS-ester peak at 2.81 ppm and the appearance of a broad peak at 4.4 ppm integrating to ~15 H, indicate the successful coupling of insulin to the endo-BCN-PEG$_4$-NHS-ester.

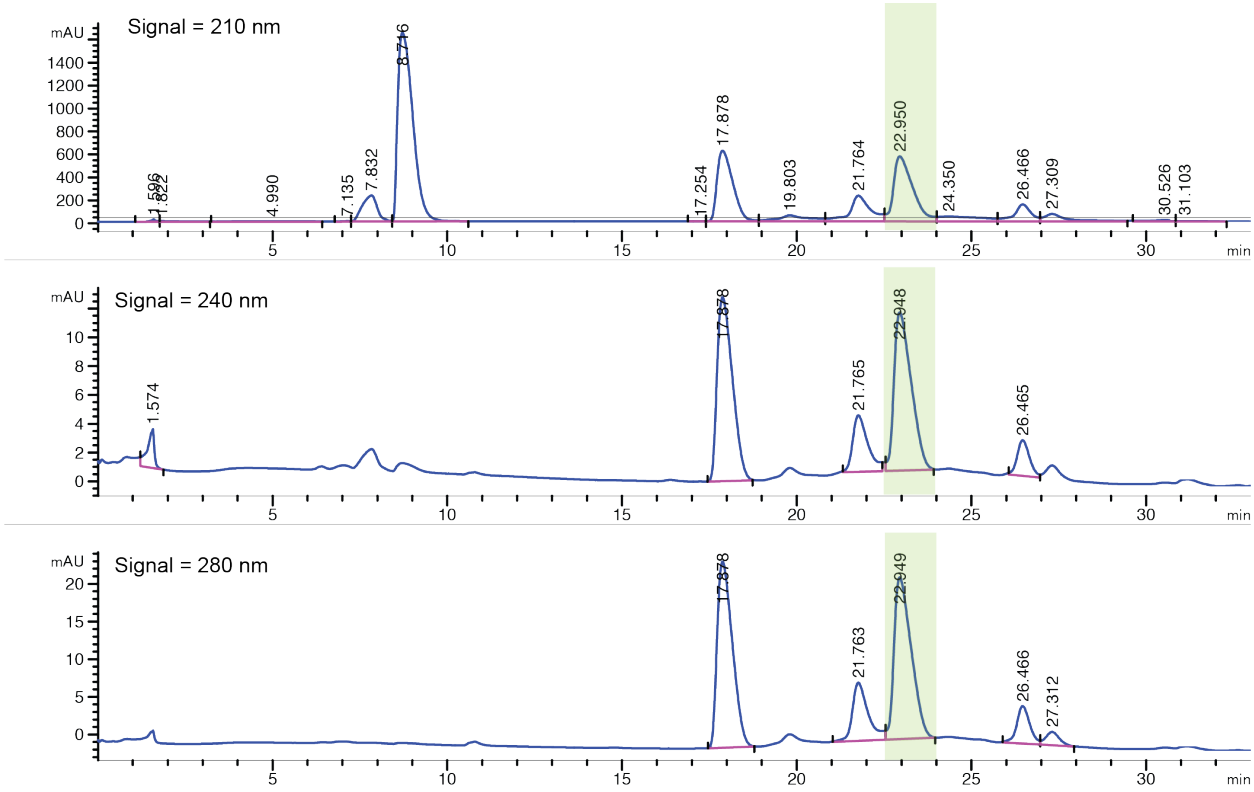

Figure S17. Purification of Insulin-BCN by HPLC. HPLC elution profile with signals shown at 210 nm, 240 nm, and 280 nm. Semi-preparative reverse-phase HPLC (Agilent 1260) was run using a C18 column with dH_2O and acetonitrile. The insulin-BCN conjugate eluted at approximately 22 minutes (peak highlighted in green).

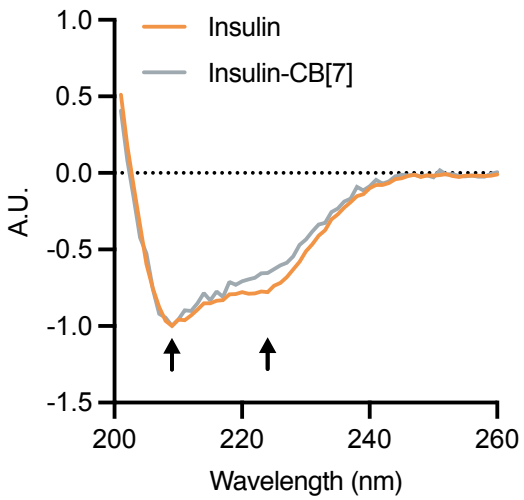

Figure S18. Circular dichroism. Circular dichroism spectra from 200-260nm for a, insulin and b, insulin-CB[7]. Curves are normalized so that the minima is at -1 (all values divided by minimum). In these experiments, insulin was diluted to 0.2mg/mL in PBS. Characteristic peaks at 223 and 208 nm are conserved in insulin-CB[7] conjugate (indicated by arrows). Prior to measurement, formulation samples were diluted to 0.2 mg/mL in PBS (pH=7.4). Samples were left to equilibrate for 15 minutes at room temperature before measurement. Near-UV circular dichroism spectroscopy was performed at 20 ºC with a J-815 CD Spectropolarimeter (Jasco Corporation) over a wavelength range of 200–260 nm using a 0.1 cm pathlength cell.

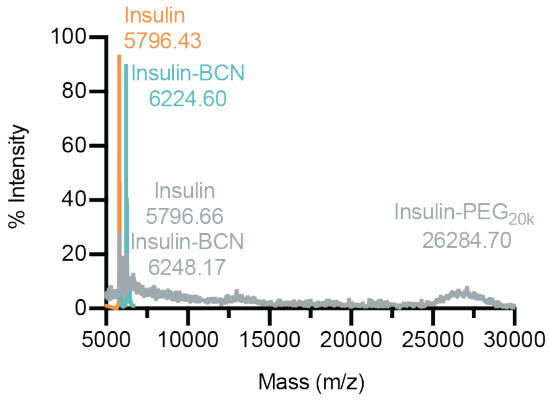

Figure S19. Insulin-PEG_{20k} MALDI. MALDI was used to verify the final products for insulin-PEG_{20k}. MALDI spectra were baseline corrected, where the minimum intensity value in the spectra was subtracted from all other values.

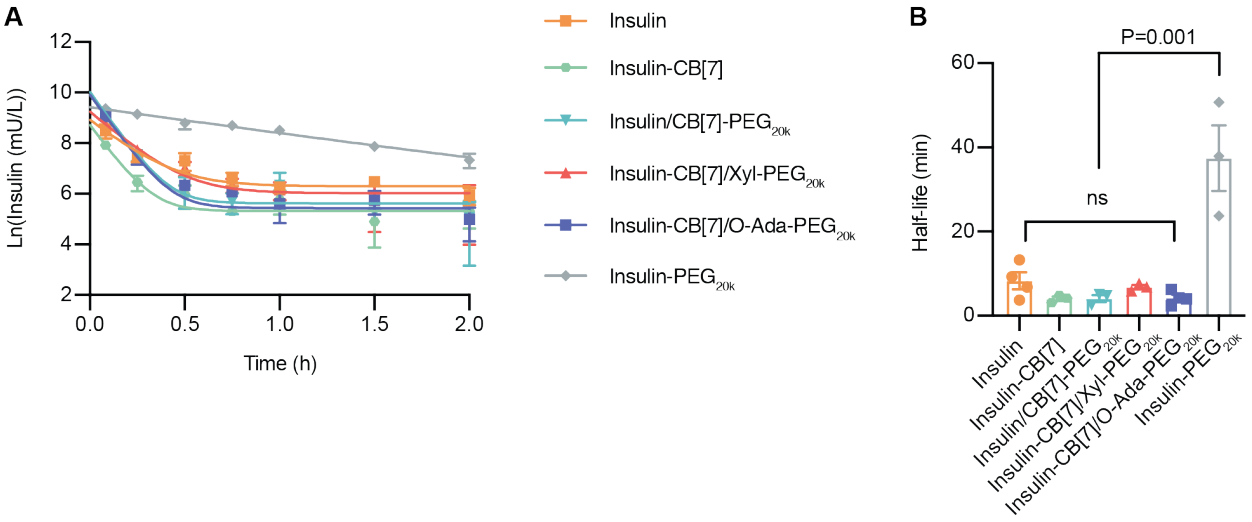

Figure S20. Pharmacokinetics following intravenous administration. Fasted diabetic rats were administered one of six insulin formulations intravenously (i) insulin (2 U/kg), (ii) insulin-CB[7], (iii) insulin/CB[7]-PEG$_{20k}$ (2 U/kg), (iv) insulin-CB[7]/Xyl-PEG$_{20k}$ (2 U/kg), (v) insulin-CB[7]/O-Ada-PEG$_{20k}$ (2 U/kg), (vi) insulin-PEG$_{20k}$ (2 U/kg). Following administration rats were given access to food. **(A)** Mean serum insulin concentrations following administration fit with a one-phase exponential decay non-linear regression. **(B)** Half-lives for each formulation calculated based on individual one-phase exponential decay non-linear regression. All data is shown as mean ± s.e.m. Comparisons of half-lives was analyzed using a one-way ANOVA with a Tukey-Kramer multiple comparisons correction (GraphPad Prism 8).

Table S1. Equilibrium, association and dissociation constants

Guest	K_{eq} (M^{-1})	k_{on} (c)[a]	k_{off} (s^{-1}) [b]	τ (s)[c]
Insulin N-terminal phenylalanine	10^6 M^{-1}	10^7 M^{-1} s^{-1}	10^1 s^{-1}	0.1 s
Xyl-PEG_{20k}	10^9 M^{-1}	10^7 M^{-1} s^{-1}	10^{-2} s^{-1}	100 s
O-Ada-PEG_{20k}	10^{10} M^{-1}	10^7 M^{-1} s^{-1}	10^{-3} s^{-1}	1000 s

[a] Complexation between CB[7] and guest has been estimated to occur with dynamics near the diffusion limit, with slower complexation occurring in the presence of cations (i.e. salt concentrations in serum) attributed to competition between the cation and guest for the CB[7] host site.[1-3] Thus, the association rate at can be approximated (k_{on} ~ 10^7 M^{-1} s^{-1}).[1-3]

[b] The equilibrium constant (K_{eq}) is related to the association constant (k_{on}) and the dissociation constant (k_{off}) as follows: $K_{eq} = k_{on}/k_{off}$. Thus, to calculate the dissociation constant the following relationship applies: $k_{off} = k_{on}/K_{eq}$. If we estimate that $k_{on}=10^7$ then values for k_{off} can be calculated based on estimates of the equilibrium constant reported in the literature.

[c] Bond lifetime (τ), is inversely related to the dissociation rate k_{off} and was calculated based on the following relationships and assumptions : $K_{eq} = k_{on}/k_{off}$; k_{on}~10^7; $\tau = 1/k_{off}$.

Table S2. Rate constants determined from model fit

Formulations	Model fit k_1	Model fit k_2	Input k_3[a]
Insulin	4.53 h^{-1}	6.27 h^{-1}	7.45 h^{-1}
Insulin/CB[7]-PEG_{20k}	0.83 h^{-1}	6.27 h^{-1}	7.45 h^{-1}
Insulin-CB[7]/Xyl-PEG_{20k}	0.32 h^{-1}	6.27 h^{-1}	7.45 h^{-1}
Insulin-CB[7]/O-Ada-PEG_{20k}	0.13 h^{-1}	6.27 h^{-1}	7.45 h^{-1}

[a] calculated from average of formulation half-lives

References:

1. Tang, H.; Fuentealba, D.; Ko, Y. H.; Selvapalam, N.; Kim, K.; Bohne, C., Guest binding dynamics with cucurbit[7]uril in the presence of cations. *J. Am. Chem. Soc.* **2011,** *133* (50), 20623-20633.
2. Miskolczy, Z.; Biczók, L., Kinetics and Thermodynamics of Berberine Inclusion in Cucurbit[7]uril. *The Journal of Physical Chemistry B* **2014,** *118* (9), 2499-2505.
3. Hu, C.; Grimm, L.; Prabodh, A.; Baksi, A.; Siennicka, A.; Levkin, P. A.; Kappes, M. M.; Biedermann, F., Covalent cucurbit[7]uril–dye conjugates for sensing in aqueous saline media and biofluids. *Chemical Science* **2020,** *11* (41), 11142-11153.